Cross-Roll Flow Forming of ODS Alloy Heat Exchanger Tubes For Hoop Creep Enhancement

Final Technical Report
October 1st 2003 – September 30th 2007

Principal Investigator:

Bimal K. Kad
Department of Structural Engineering
University of California-San Diego, La Jolla, CA 92093-0411
Tel: (858) 534 7059; Fax: (858) 534-6373; e-mail: bkad@ucsd.edu

Issue Date: March 31st 2008

National Energy Technology Laboratory
Contract Award: DE-FC26-03NT41985

For

Development of Technologies and Capabilities for Developing Coal, Oil and Gas Energy Resources

Cross-Roll Flow Forming of ODS Alloy Heat Exchanger Tubes For Hoop Creep Enhancement

Abstract

Mechanically alloyed oxide dispersion strengthened (ODS) Fe-Cr-Al alloy thin walled tubes and sheets, produced via powder processing and consolidation methodologies are promising materials for eventual use at temperatures up to 1200^{o}C in the power generation industry, far above the temperature capabilities of conventional alloys. Target end-uses range from gas turbine combustor liners to high aspect ratio (L/D) heat exchanger tubes. Grain boundary creep processes at service temperatures, particularly those acting in the hoop direction, are the dominant failure mechanisms for such components. The processed microstructure of ODS alloys consists of high aspect ratio grains aligned parallel to the tube axis, a result of dominant axial metal flow which aligns the dispersoid particles and other impurities in the longitudinal direction. The dispersion distribution is unaltered on a micro scale by recrystallization thermal treatments, but the high aspect ratio grain shape typically obtained limits transverse grain spacing and consequently the hoop creep response. Improving hoop creep in ODS-alloy components will require understanding and manipulating the factors that control the recrystallization behavior, and represents a critical materials design and development challenge that must be overcome in order to fully exploit the potential of ODS alloys.

The objectives of this program were to 1) increase creep-strength at temperature in ODS-alloy tube and liner components by 100% *via*, 2) preferential cross-roll flow forming and grain/particle fibering in the critical hoop direction. The research program outlined was iterative and intended to systematically i) examine and identify post-extrusion forming methodologies to create hoop strengthened tubes, to be ii) evaluated at 'in-service' loads at service temperatures and environments.

Our report outlines the significant hoop creep enhancements possible via secondary cross-rolling and/or flow-forming operations. Each of the secondary processes i.e. hot rotary forming and ambient-temperature flow forming exhibited improvement over the base-line hoop-creep performance. The flow formed MA956 tubes exhibited performance superior to all other rolling/forming variants. At the conclusion of this program 2ksi creep-test exposure for flow formed materials exceeded 7300 hours, 7694 hours and 4200 hours for creep tests operating at 950^{o}C, 975^{o}C and 1000^{o}C respectively. The Larsen-Miller parameter for these improvised flow-formed tubes now exceeds 54.14, *i.e.*, better than ever recorded previously. The creep performance enhancement in cross-rolled MA956 material samples versus the base creep property is elucidated. ***At least 2-3 orders of magnitude of improvement in creep rates/day and concomitant increases in creep-life are demonstrated for the flow formed tubes versus the base reference tests.***

Cross-Roll Flow Forming of ODS Alloy Heat Exchanger Tubes For Hoop Creep Enhancement

Table of Contents

Cross-Roll Flow Forming of ODS Alloy Heat Exchanger Tubes For Hoop Creep Enhancement

List of Figures

§ 1. Executive Summary

Mechanically alloyed oxide dispersion strengthened (ODS) ferritic alloys based on FeCrAl and intermetallic Fe3Al alloys are promising materials for high-temperature, high-pressure tubing, liner and shell applications on account of their creep strength at very high temperatures and excellent corrosion resistance in oxidizing, oxidizing/sulphidizing and oxidizing/chlorinating environments compared to available high-temperature alloys. Requirements for such a combination of properties are found in advanced systems being developed for utilization of fossil fuels, such as the **DOE**'s **Vision 21** and **FutureGen** programs and in improved gas turbines being developed for power generation.

The creep strength of conventional high-temperature alloys decreases rapidly with increasing temperature, as shown in Fig. 1, since the thermodynamic stability of the various available strengthening phases also decreases with increasing temperature[1]. Also shown in Fig. 1 is the significant increase in temperature capability afforded when a dispersion of inert oxide particles is used as the strengthening phase. A major feature of oxide dispersion-strengthened alloys is that the most successful route for their preparation appears to involve powder metallurgical processing[2-6]. Further, the critical need to maintain the fine size, volume fraction, and uniform distribution of the oxide particles in the alloy matrix, as well as the need to develop specific grain shapes, results in some significant differences in alloy fabricability and in the application of joining procedures, compared to conventional cast and wrought alloys. Hence, while ODS alloys offer a significant increase in temperature capability, they have a limited formability envelope, their mechanical properties are very anisotropic, and they cannot be joined by conventional fusion welding processes. Thus, the exploitation of the full capabilities of ODS alloys is limited until these critical hurdles are addressed and overcome.

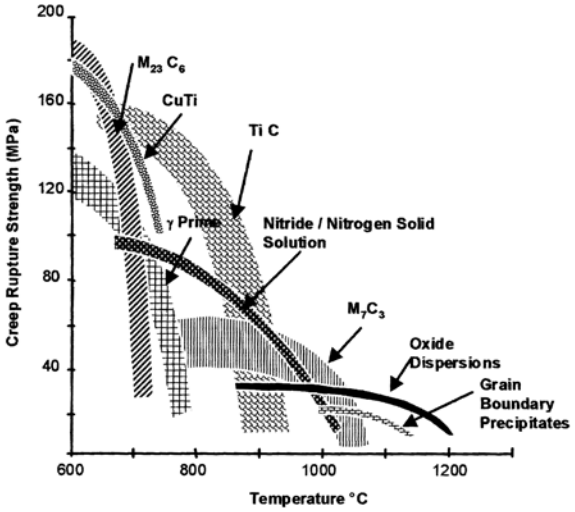

Figure 1. The creep performance envelope as a function of strengthening phase [1].

This current program was designed as a demonstration of the applicability of ferritic and Fe_3Al-based ODS alloys in the high temperature heat-exchanger tubing as proposed under the proposed **DOE's Advanced Power System** program metrics, intended to sustain internal pressures (P) of up to 1000psi at service temperatures of 1000-1200^{O}C. Within the framework of this target application, the development of suitable mechanically alloyed ferritic FeCrAl and intermetallic Fe_3Al alloy materials and processes must strive to deliver a combination of high mechanical strength at temperature and prolonged creep-life in service. Such design requirements are often at odds with each other as strengthening measures severely limit the as-processed grain size detrimental to creep life. The extrusion consolidation processes currently employed cause material flow in the longitudinal direction, resulting in extreme dispersoid and powder surface impurity fibering in the axial direction in ODS materials. Thus, elongated grains are produced aligned parallel to the longitudinal direction, with a fine grain spacing in the hoop direction. The basic problem of limited hoop creep is illustrated in Figure 2a,b within the context of the existing underlying grain structure. Fortunately ODS-alloys do exhibit intrinsic creep

strength sufficient to meet design requirements albeit that this performance is only exhibited in the longitudinal direction. Ultimate failure in transverse (hoop) creep involves creep cavity concentration, Figure 2b, which strongly depends on the dominant grain boundary orientation with respect to the loading axis, Figure 4[7]. Such fibering, unless altered by post-flow forming, is expected to thwart attempts to arrive at the large transverse grain size[3,8] considered essential for improved creep performance in the hoop direction. Clearly what is required is to devise a means of effecting material flow in directions other than longitudinal that would reorient the primary fibering axis of dispersoids and impurities in the hoop direction.

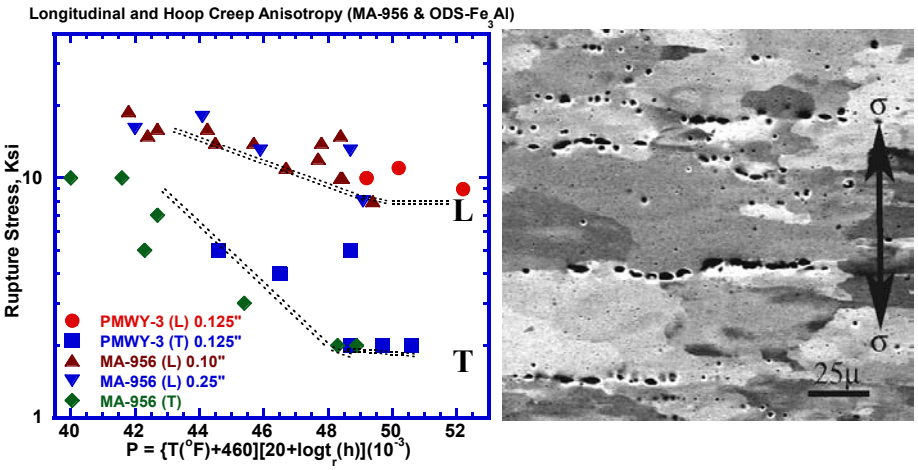

Figure 2. Longitudinal (L) vs. transverse (T) creep anisotropy in Fe_3Al (PMWY3) and MA-956 tubes. b) Creep cavitation observations in hoop creep loading tests.

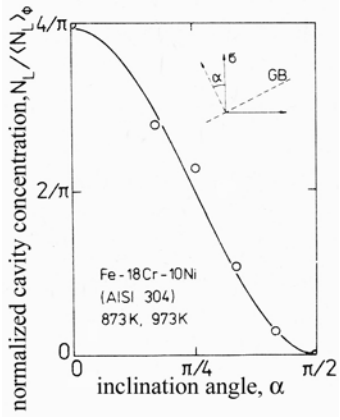

Figure 3. Creep cavity density as f_n(GB orientation) with respect to the loading axis [7].

Thus, our research objective was to modify tube-processing methodologies by incorporating cross-roll forming to create the underlying microstructure that will meet or exceed the design 'in-service' hoop creep-life requirements of such ODS-alloy heat exchanger tubes. We examined microscopic, microstructural and morphological issues with a view to addressing optimum material design for macroscopic components for a well prescribed 'in-service' loading criteria.

Our report outlines the significant hoop creep enhancements possible via secondary cross-rolling and/or flow-forming operations. Each of the secondary processes i.e. hot rotary forming and ambient-temperature flow forming exhibited improvement over the base-line hoop-creep performance. The hot cross-rolled tubes, processed under separate configurations (labeled $\beta = 2^o$ and $\beta = 8^o$) provided consistent improvement in hoop creep performance. The cross-section microstructure indicated the circumferential stretching of the grains. This preferred grain shape structure was resistant to secondary recrystallization. However, the ambient temperature flow formed MA956 tubes exhibited performance superior to all other rolling/forming variants. Such tubes underwent much greater extent of cold-work, and could be readily recytsallized into large grains. At the conclusion of this program 2ksi creep-test exposure for flow formed materials exceeded 7300 hours, 7694 hours and 4200 hours for creep tests operating at 950°C, 975°C and 1000°C respectively. The Larsen-Miller parameter for these improvised flow-formed tubes now exceeds 54.14, *i.e.*, better than ever recorded previously. The creep performance enhancement in cross-rolled MA956 material samples versus the base creep property is elucidated. ***At least 2-3 orders of magnitude of improvement in creep rates/day and concomitant increases in creep-life are demonstrated for the flow formed tubes versus the base reference tests.***

§ 2. Experimental Task Structure

The experimental work proposed was divided into main four main tasks as outlined.

Task 1: Extrusion Consolidations, Tube and Sheet Forms:

1.1 ODS-Powder materials –milling studies, impurity evaluation
1.2 Annular ODS-Alloy tube and sheet extrusions

Task 2: Rolling Studies for Optimum Fibering:

2.1 Single vs. cross-rolling evaluation, Parametric studies
2.2 Correlate cross-rolling strains and overall grain re-orientation

Task 3: Post-Extrusion Cross-Roll Rolling of ODS-tubes & shells:

3.1 Helical/cross rolling for grain fibering
3.2 Computer model verification for torsional flow predictions

Task 4: Microstructure and Creep Performance Evaluation:

4.1 Recrystallization annealing: static and gradient
4.2 Microstructure characterization & evaluation
4.3 Transverse creep and stress-rupture response

§ 3. Experimental Activities and Results

Task 2: Single vs. cross-rolling evaluation, parametric studies

Conventional extrusion consolidation processes currently employed cause material flow in the longitudinal direction, resulting in extreme dispersoid and powder surface impurity fibering in the axial direction in ODS materials. Thus, elongated grains are produced aligned parallel to the longitudinal direction, with a fine grain spacing in the hoop direction. The resulting creep anisotropy in longitudinal versus transverse (hoop) directions was illustrated in Figure 1(a). Thus, the initial objective of laboratory scale cross-rolling was to experimentally demonstrate that a preferential grain shape change in the transverse direction would subsequently improve performance in the transverse direction.

ODS materials produced via extrusion consolidation in Task 1 (or procured) were sectioned and examined for microstructural details. The ODS MA956 tubes of 2-½" OD, ¼" wall thickness was procured from Special Metals Corporation. A flattened tube strip was the required material for the initial matrix of parametric cross-rolling studies. Thus, the ODS alloy tubes were longitudinally sectioned and forge-flattened via a 900^{o}C thermal-mechanical treatment for subsequent cross-rolling studies. No recrystallization was observed in either alloy materials as a result of this 900^{o}C thermal-mechanical treatment. Based on the post-forging microstructural evaluation, and in the interest of narrowing experimental windows, all further cross-rolling studies were conducted at 900^{o}C.

Residual curvature in the forge-flattened specimens was eliminated via subsequent rolling prior to any cross-rolling rolling deformations. Three separate rolling steps were employed:

1) Rolling longitudinally in 0.01" steps till the sample was measurably flat,

2) Rolling transversely to the tube axis in 0.01" steps till the sample was measurably flat, and

3) Rolling transversely for 20-25% thickness reduction in the starting ¼" wall thickness.

All rolling steps were accomplished by preheating the specimen at 900°C for 15 minutes in the air furnace. In the rolling schedule 3, this large deformation was accomplished in steps of 4-5% reduction per pass with the sample reheated at 900°C for 15 minutes in the air furnace between passes. The flat rolled samples were removed from their stainless steel wraps and prepared for the recrystallization treatments. The cross-rolled specimens were recrystallized to create secondary grain growth in such ODS-alloy tube coupons. The heat treatments were 1-hour at 1200°C in air for ODS-Fe_3Al and a 1-hour at 1375°C in air for MA956 tube coupons. Both materials exhibit primary recrystallization but secondary grain growth was observed only in ODs-Fe3Al coupons resulting in large grains. Microstructures reveal elongated grain shapes in the transverse orientation only for the sample cross-rolled 20-25% in the transverse orientation. It is likely that surface layers are affected in rolling schedule 1 and 2 outlines above but no grain shape changes are perceptible at the optical resolution level.

Task 3: Rotary Cross-Roll Rolling of Tubes

The challenge in this task is to explore methodologies to impart the beneficial aspects of cross-rolling as performed in Task 2 to ODS alloy tubes. Such ODS tubes currently exhibit poor hoop creep performance and will be benefit from any improvements in their creep response.

Figure 4 provides the essential schematic of the mandrel piercing tube rolling process, which is used in seamless tube manufacturing of conventional alloys. The principal difference to conventional rolling apparatus is that the rolls are set obliquely to each other and are inclined at small but equal angles (α) to the tube feed axis (z). The surface velocity of the roll (V_t) at any material contact point is decomposed into V_{tz} in the longitudinal direction, and $V_{t\theta}$ in the circumferential direction, as given by:

$$V_{tz} = V_t \sin \alpha = \omega R_{\omega z} \sin \alpha \quad (1)$$
$$V_{t\theta} = V_t \cos \alpha = \omega R_{\omega z} \cos \alpha \quad (2)$$

where ω = angular velocity of the rolls, and $R_{\omega z}$ is the roll radius at the section of interest. The hollow tube is subjected to the action of frictional traction forces, whereby the axial component produces the forward movement of the tube, and the tangential component produces cross-rolling and is responsible for its torsional rotation[13]. This tangential component is akin to the rolling pressure applied in Task 2.

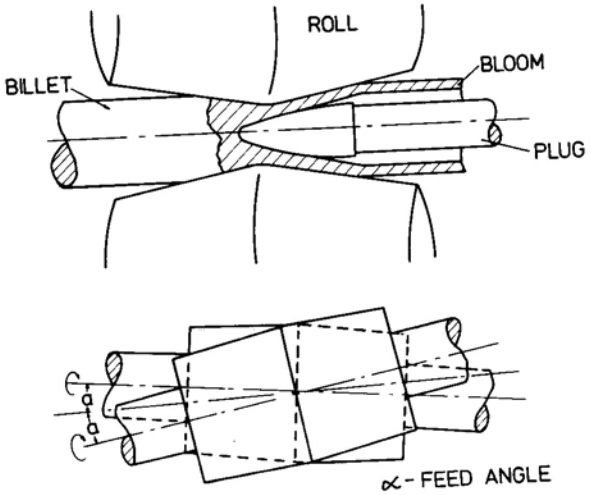

Figure 4. Tube cross-rolling schematic. The surface inclination of the rolls and the feed angle α dictate the overall circumferential strain and torsion.

Cross-rolling trial experiments are typically performed employing two main variables. a) Rolling pressure and b) the rolling angle (α). The machine class and the size of the power plant turning the rolls under pressure dictate rolling pressure. The rolling angle provides the force bifurcation into the normal pressure component and the translation component affecting the movement of the tube through the roll gap geometry. As part of this task UCSD purchased, reconditioned and installed a rotary cross-rolling set up for all cross-rolling operations of MA956 and ODS-Fe_3Al tubes under this program and any future needs. Figure 5 shows a Medart size '0' straightener currently installed at UCSD. The modified size '0' machine, powered by a 30HP motor, is capable of processing rod and bar in the size range of ¼" – 1½" and tubes in the size range ¼" – 2½". at near ambient temperatures in MA956 alloys.

Figure 5 Cross-Rolling equipment currently installed at UCSD. The equipment is capable of rolling up to 1-1/2" bar/rod and up to 2-1/2" diameter alloy tubing in a continuous fashion

Figure 6 Hot rotary cross-rolling of ODS MA956 tubes

Figure 7 Surface markings on ODS MA956 tubes cross rolled at oblique ß=2° (top) and ß=8 °.(bottom).

Rotary cross rolling trials of 12" long MA956 tube sections were attempted at rolling angles of 2° and 8° at a rolling temperature of 900°C. Tubes were preheated at 900°C in an air furnace and loaded onto a mandrel and rolled through the convex-convex roll setup, Figure 6. The reversible rolling setup allows for rolling in the forward and reverse rolling at each pass. A total of 6-10 passes are given through the rolls reheating the tube after each pass for 10 minutes. Note that precise measurements of rolling pressure are not possible but the roll gap and subsequent roll gap increments are kept consistent over the series of experiments performed. Figure 7 shows

the surface markings for the β=2° (top) and β =8° (bottom) deformation indicative of the forward travel pitch for the respective oblique roll settings. Figure 8 shows the corresponding end view of the tube walls after the β=2° (top) and β =8° (bottom) deformation. A measure of the overall rolling deformation was extracted as follows: a straight radial (dashed red line) notch was inscribed on the tube wall prior to cross-rolling to monitor material flow during the deformation process. The inclined image of the same notch (indicated by red arrows) provides a measure of the shear deformation induced by rotary cross rolling. We note that the notch is remarkably straight for the β=8° rolling angle condition indicating that the shear deformation is rather uniform over the entire tube wall thickness. Shear deformation is non-uniform and confined to the middle of the tube wall section for β=2° rolling angle. The shear angle (γ) measured as 35° (in Figure 8, bottom) with a shear strain = 0.7 similar to transverse rolling strains in Task 2.

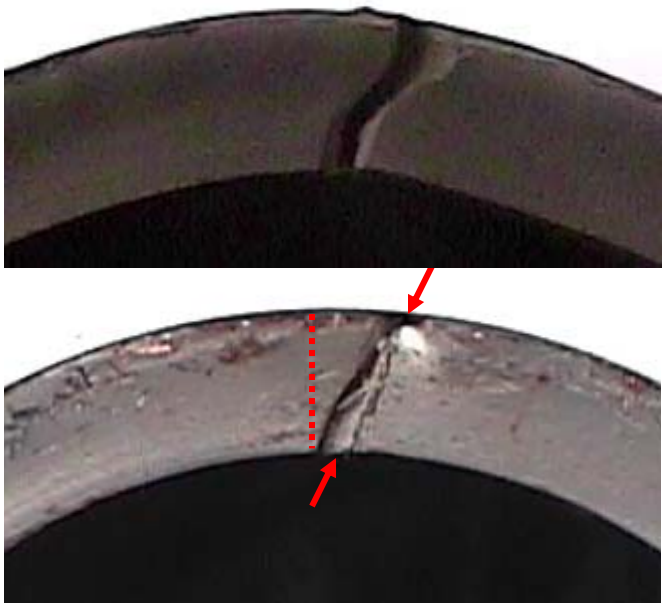

Figure 8. Cross rolling of MA956 tube via repeated passes at 900°C. Micrographs show rolling angle β=2° (Top) and 8° (Bottom). The red line indicates the notch as inscribed on the tube wall prior to testing. The angle between the red line and the sheared image (denoted by red arrows) gives the shear strain incurred via rotary cross-rolling process.

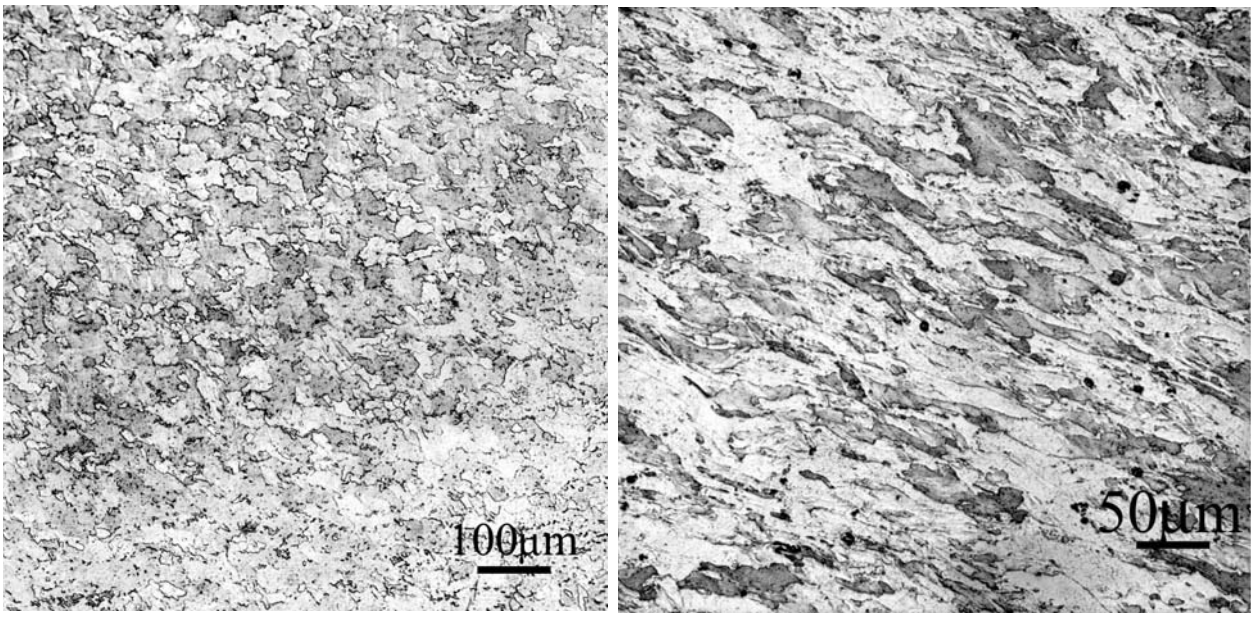

Figure 9. Cross-sectional view of a) as –received, recrystallized and b) cross-rolled and recrystallized MA956 tube (β=8°). The grain shape is significantly modified, with the long axis now stretched along the hoop direction.

Figure 9 (a), (b) show the before and after tube cross-section views indicating grain realignment under such rotary cross-rolling deformation. The as-received MA956 tube typically shows an equi-axed grain structure in the tube wall cross-section, Figure 9a. This initial grain

structure undergoes a shape change under rotary deformation, Figure 9(b). The grains with their aspect ratio significantly greater than unity and extended in the circumferential (hoop) direction are deemed beneficial for hoop creep performance.

Alternate forming processes: Unrecrystallized MA956 tubes flow formed at ambient temperatures under a separate DOE program with Special Metals Corporation were made available for microstructure evaluation and high temperature testing. The flow-forming, performed in several steps, resulted in tube wall thickness reduction of 80-90%. It was originally surmised that flow-forming would create grain re-orientations along the circumference[10], though not realized and could not be verified here. High temperature testing of flow formed tubes was incorporated into our prescribed testing program. As shown later, this provides important insight into processes that may affect the overall creep performance.

Task 4: Recrystallization Microstrutures and High Temperature Creep Properties:

The thermal-mechanical forming of Task 2 and Task 3 are performed on un-recrystallized MA956 tubes. The preference for un-recrystallized tubes is on account of their greater formability which is severely diminished upon recrystallization. However, materials for creep environments benefit from coarse microstructures. Thus, the post extrusion deformed tubes and plates of Task 2 and task 3 are subjected to primary and secondary recrystallization strategies for creating abnormal grain growth in ODS alloy materials. Table 1 lists the recrystallization heat-treatments for the ODS Fe_3Al and MA956 alloys.

Table 1: Recrystallization matrix for cross-rolled ODS-Fe3Al and MA956 materials

HT Test#	Material	HT: Temperature, ^oC	HT: Time, Hrs	Environment
1	ODS-Fe_3Al	1200^{o}C	1 hr	Air
2	ODS-Fe_3Al	1200^{o}C	1 hr	Argon
3	ODS-MA956	1375^{o}C	1hr	Air
4	ODS-MA956	1400^{o}C	1hr	Air

The heat-treatment temperatures are based on prior DOE funded work[2-5] performed by the PI. The introduction of inert environment heat treatment was initially applied to ODS-Fe_3Al alloys[3,8], which produced significant improvements in transverse creep. The 1375^{o}C heat treatment for MA956 was prescribed by the material vendor SMC. In the current program a 1400^{o}C heat treatment was attempted to promote secondary grain growth but was later discontinued on account of the aggressive oxide formation at the elevated temperatures.

Task 4.2: Microstructure Evaluation: The recrystallized microstructures of as-received MA956 tubes reveal elongated grain shapes in the longitudinal direction, Figure 10(a), and a near equi-axed grain shape in the tube wall cross-section, Figure 9(a). This microstructures produced following Task 4.1 treatments is consistent with the expected grain structure. The recrystallized microstructure of the modified grain shape produced via rotary cross rolling was elucidated earlier in Figure 9(b). We note that no large scale secondary recrystallization was observed before or after the rotary cross-rolling processes of Task 3, and despite the obvious grain shape change the mean grain size is reasonable similar and small, of the order of 50-100μm in the transverse direction.

One beneficial aspect of post extrusion processing is to mitigate the existence of unrecrystallized stingers of fine-grained material dispersed through out the matrix. Figure 10(a) shows the stringers (indicated by arrows) stretched along the extrusion axis. The stringers are

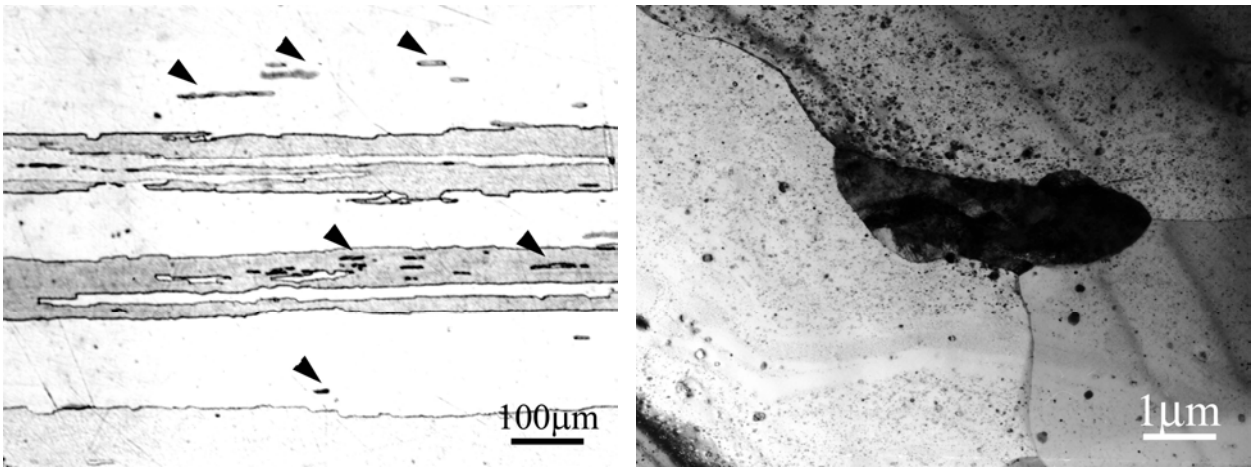

Figure 10 a) optical micrograph of as-extruded and recrystallized MA956 with a large number of unrecrystallized stringers, which are mitigated via secondary processing though b) not entirely eliminated, TEM

normal to the hoop creep loading and consequently detrimental to hoop creep performance. Looking back to Figure 2(b) creep failure occurs by void formation at grain junctions and boundaries and stringers located in the grain boundary vicinity, Figure 10(b), may be particularly susceptible. Such stringers are minimized (i.e. reduced in size and in numbers) via post processing working though not entirely eliminated. Figure 10(b) shows the remnant of such stringers in cross-rolled materials, where they exist at grain boundaries or within a single grain.

Task 4.3: Transverse Creep and Stress Rupture Response: The initial flat cross-rolled samples from Task 2, the rotary cross-rolled samples from Task 3 were heat treated in Task 4.1 and prepared for high temperature transverse (hoop) creep testing. Tube samples are initially flattened at 900°C using a combination of hot pressing and rolling. ASTM E-8 specimens li; lkop,.lopare then extracted via electrical discharge machining in the transverse orientation from the tube wall-thickness. All materials are evaluated in transverse creep tests performed at dead load 1-2Ksi stresses over a temperature range of 800°C –1000°C in air.

Figure 9 shows the typical response of MA956 samples flat cross-rolled (cross rolled 20% in Task 2) in creep tests. The sample exhibits a brief primary regime, an extended steady state regime (creep rate=$9e^{-5}$/day) followed by a tertiary regime. The y-axis gridline spacing denotes a creep strain of 2%. Note that the sample fails at an overall strain of about 3% with the largest component of strain (about 2%) occurring in the tertiary (failure) regime. The transverse creep strain life is estimated at under 1% and the mean steady state creep-rate/day is used as a simple measure of expected life at service temperatures. The creep life (Larsen-Miller parameter) LMP = 48.87 based on 1381hrs test exposure) is of the order of about 1% creep strain in the steady-state regime.

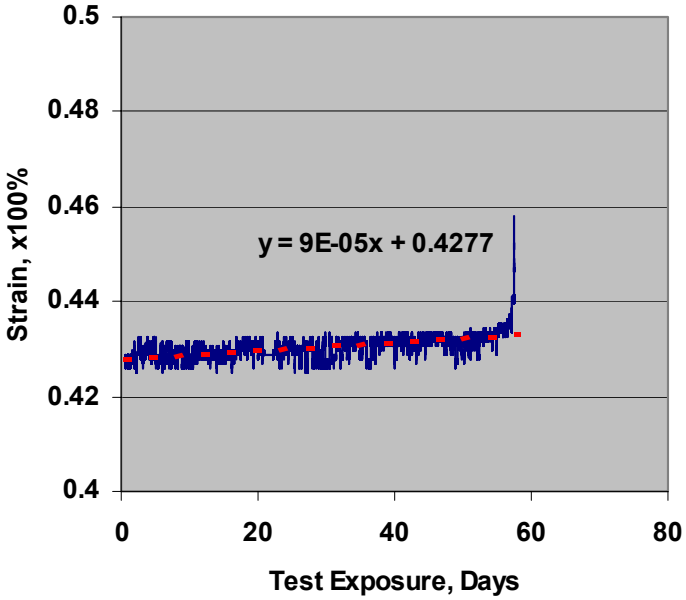

Figure 11. Creep test of MA956 sample extracted from a 2 ½" OD, ¼" wall thickness tube and cross-rolled at 900°C to 20% reduction. Creep test conducted at 900°C at 2Ksi stress in air.

Table 2 lists selected creep data compiled for as-received MA956 base material (Test# 1-3), flat cross-rolled samples of Task 2 (Test# 4-7) and the rotary cross-rolled samples (Test# 8-13) from Task 3. Samples for the base property evaluation and the cross-rolling experments were all extracted from the same 2½"OD, ¼" wall thickness MA956 tube. Similar MA956 tubes are used for flow forming where the wall thickness is reduced 75-80% in several reducing steps at ambient temperatures. Base material tests 1-3 were run at 900-950^{o}C in air at a 1-2Ksi stress. The recorded Larsen-Miller (L-M) Parameter for the base material is rather poor. In comparing tests 1-3 we note both an acute stress and temperature sensitivity in this upper limit temperature regime. For example, the creep rate at 900^{o}C increases by three orders of magnitude from 2.0e^{-5} to 2.0e^{-2} when the stress is incremented from 1Ksi to 2Ksi, and increases by about two orders of magnitude from 2.0e^{-5} to 1.5e^{-3} as temperature is increased from 900^{o}C to 950^{o}C at constant stress of 1Ksi. A peak value of L-M = 46.09 at a mean creep-rate of 2.0e^{-2} was observed for test# 1 loaded at 2Ksi and is used for all future base material comparisons. The mean creep rate/day (for tests 4-6) is estimated at 1.75e^{-4} with a mean Larsen Miller parameter = 48.67. *Thus, at least 2 orders of magnitude improvement in creep rates is achieved for the cross-rolled tests in this initial evaluation*. Test 7 indicates the strain rate sensitivity with respect to temperature. Thus strain rate drops by about 3 orders of magnitude from 1.0e^{-4} range to 6.0e^{-7} as the temperature is lowered from 900^{o}C to 800^{o}C. This test was terminated after 3400 hours as the creep-strain was observed to saturate at this temperature.

Table 2. Summary of creep tests performed on cross-rolled and base MA956 alloy tubes

Test	MA956 Alloy Treatment & HT	Test Temp	Test Stress	L-M Para.	rate/day
1	Flattened@900C,HT: 1375^{o}C-1hr,Air	**900^{o}C**	**2Ksi**	**46.09**	**2.00e^{-2}**
2	Flattened@900C,HT: 1375^{o}C-1hr,Air	**900^{o}C**	**1Ksi**	**48.81**	**2.00e^{-5}**
3	Flattened@900C,HT: 1375^{o}C-1hr,Air	**950^{o}C**	**1Ksi**	**49.20**	**1.50e^{-3}**
4	CR-20%@900C,HT: 1375^{o}C-1hr,Air	**900^{o}C**	**2Ksi**	**48.87**	**9.00e^{-5}**
5	CR-20%@900C,HT: 1375^{o}C-1hr,Air	**900^{o}C**	**2Ksi**	**48.24**	**6.00e^{-4}**
6	CR-20%@900C,HT: 1400^{o}C-1hr,Air	**900^{o}C**	**2Ksi**	**48.89**	**1.00e^{-4}**
7	CR-20%@900C,HT: 1400^{o}C-1hr,Air	**800^{o}C**	**2Ksi**	**-***	**6.00e^{-7}**
8	CR@900C, β=8^{o}, HT:1375^{o}C-1hr,Air	**1000^{o}C**	**2Ksi**	**48.31**	**1.00e^{-1}**
9	CR@900C, β=8^{o}, HT:1375^{o}C-1hr,Air	**950^{o}C**	**2Ksi**	**46.84**	**6.00e^{-2}**
10	CR@900C, β=8^{o}, HT:1375^{o}C-1hr,Air	**950^{o}C**	**2Ksi**	**46.80**	**7.00e^{-2}**
11	CR@900C, β=8^{o}, HT:1375^{o}C-1hr,Air	**925^{o}C**	**2Ksi**	**46.86**	**1.90e^{-2}**
12	CR@900C, β=8^{o}, HT:1375^{o}C-1hr,Air	**900^{o}C**	**2Ksi**	**46.89**	**5.70e^{-3}**
13	CR@900C, β=8^{o}, HT:1375^{o}C-1hr,Air	**875^{o}C**	**2Ksi**	**46.90**	**1.20e^{-3}**

Tests 8-13 in Table 2 provide the corresponding hoop creep performance of hot rotary cross rolled tubes (from Task 3). The process of extracting specimens from these tubes is essentially similar to that described earlier. Test 8 yields enhanced creep performance for a 1000^{o}C test loaded to 2ksi stress, though the observed test life was small. The testing temperature was subsequently lowered to the 875–950^{o}C range to achieve increased exposure times as listed for tests 9-13 in Table 2. The Larsen Miller parameter (LMP) for tests 9-13 is quite consistent (i.e. between 46.84 and 46.90) and reproducible in this 875–950^{o}C temperature range. We note that the LMP enhancement while consistent is marginal. A comparison of observed creep rates/day shows the creep rate dropping from 6.e^{-2} at 950^{o}C to as low as 1.2e^{-3} at 875^{o}C. A comparison of the baseline test#1 and rotary cross rolled test# 12 (both tests performed at 900^{o}C) shows that

creep rate/day drops from $2.e^{-2}$ to $5.7e^{-3}$ suggesting that some consistent benefit is accrued and could be further improved with processing as indeed observed in tests 3-7 for the flat cross-rolled specimens of Task 2. As shown later in Table 3 significant enhancements are possible when tubes are processed at ambient temperatures.

Table 3 lists the hoop creep performance data for the ambient temperature flow-formed tubes deformed via 80-90% reduction in tube wall thickness. These flow formed tubes are initially slit by spark machining and either flattened at room temperature and recrystallized in air (Air1, tests 2-5) or flattened at 900°C and recrystallized in air (Air2, tests 7-10)

Table 3. Summary of creep tests performed on ambient temperature flow formed tubes

Test	MA956 Alloy Treatment & HT	Temp	Stress	Life, hrs	LM Para	rate/day
1	Flattened@900C,HT:1375°C-1hr,Air	900°C	2Ksi		46.09	$2.00e^{-2}$
2	FlowForm@RT,HT:1375°C-1hr,Air1	900°C	2Ksi		48.91	$5.00e^{-4}$
3	FlowForm@RT,HT:1375°C-1hr,Air1	1000°C	2Ksi		48.77	$1.14e^{-2}$
4	FlowForm@RT,HT:1375°C-1hr,Air1	950°C	2Ksi		48.60	$2.60e^{-3}$
5	FlowForm@RT,HT:1375°C-1hr,Air1	950°C	2Ksi		49.83	$4.00e^{-4}$
6	FlowForm@RT,HT:1375°C-1hr,Air1	900°C	2Ksi		49.00	$4.00e^{-4}$
7	FlowForm@RT,HT:1375°C-1hr,Air2	1000°C	2Ksi	452	51.93	$7.00e^{-4}$
8	FlowForm@RT,HT:1375°C-1hr,Air2	950°C	2Ksi	7329	52.55	$2.00e^{-5}$
9	FlowForm@RT,HT:1375°C-1hr,Air2	975°C	2Ksi	7694	53.67*	$3.00e^{-5}$
10	FlowForm@RT,HT:1375°C-1hr,Air2	1000°C	2Ksi	4200	54.14*	$2.00e^{-5}$

Examining tests 2-6 (of heat treatment Air1) we note a mean creep-rate/day of about $4.0e^{-4}$ at 900°C that rises to about $2.6e^{-3}$ at 950°C and $1.1e^{-2}$ at 1000°C. While there appears to be some scatter in the data, the test results indicate improvement over the rotary cross-rolled materials. The data suggests that L-M parameter is essentially consistent over the 900-1000°C ranges and reconfirms the validity of accelerated creep tests. We note that ambient temperature flattening of flow-formed tubes always produced samples with some residual warp in them. In particular, some residual curvature is often observed in the gage section of the ASTM E-8 specimens in test# 2-6 in Table 3.

Ambient temperature flattening was deemed desirable to preserve the large cold-forming induced strain energy into the material to help produce a large processed grain structure. However, there was some concern that the data yielded sufficient scatter and more importantly the curvature-induced effects were undermining or masking true material and microstructure performance. Thus, the thermo-mechanical flattening procedure is revised with flattening performed at 900°C (labeled Air2) in parity with other rolled specimens (i.e., in tests#1-13 in Table 2). Figure 12 illustrates the effect of thermo-mechanical treatment of flattening at

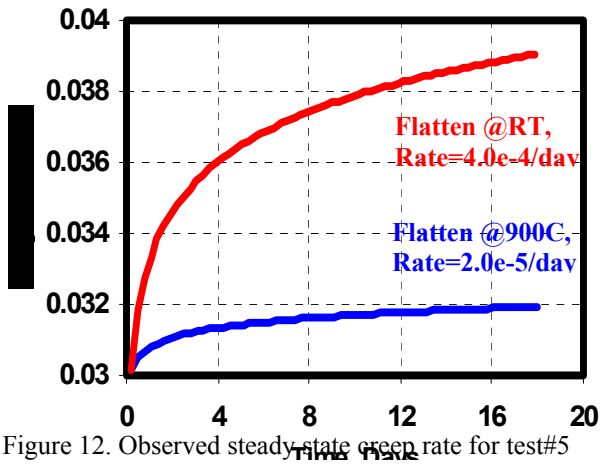

Figure 12. Observed steady-state creep rate for test#5 and 8 as a function of thermo-mechanical processing.

room temperature versus 900°C on ensuing creep rate. Sample flattened at room temperature (test#5 as depicted) exhibits both a higher primary creep strain as well as a higher creep rate in the steady state regime than a corresponding sample flattened at 900°C (test#8). The primary strain may be somewhat exaggerated because of the initial warping in the test specimens. Total exposure of 7330 hours at test temperatures of 950°C at a 2ksi stress has been achieved for Test#8. Current test #9 at 975°C and test#10 at 1000°C continue till date with exposures of 7694 and 4200 hours, respectively. Figure 13 shows the initial creep response of test#9. The creep rate moderates over time and stabilized at $3.0e^{-5}$/day averaged over the initial transient. Subsequently this creep rate falls to $1.0e^{-6}$/day range. The high temperature performance of flow-formed MA956 tubes is validated with incrementally higher reported Larsen Miller Parameter values. This revised recrystallization (Air2) scheme provides considerable gains in hoop creep response. The revised HT specimens are being tested in the 950-1000°C range and comparisons with other deformed specimens are only possible at 950°C. For example, the observed creep rate=$1.5e^{-3}$ for base material (test#3 at 1Ksi, Table 2), $4.00e^{-4}$ for flow-formed HT1 and $4.00e^{-5}$ for flow-formed HT2 treatments.

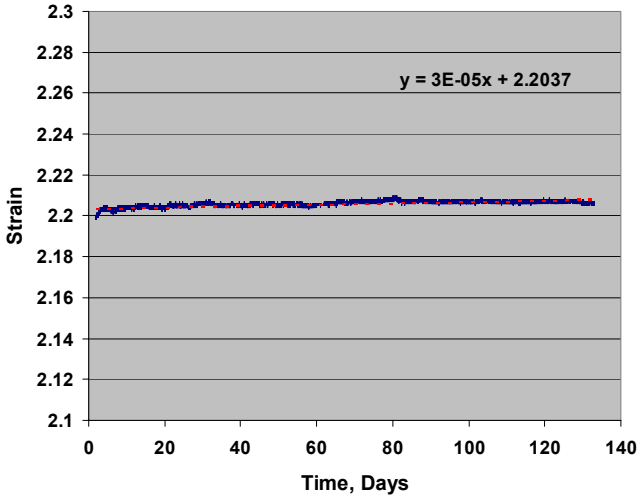

Figure 13. Initial hoop creep response for MA956 flow formed tube tested at 2Ksi load at 975°C.

§ 4. Results and Discussion

The experimental program reported herein validates the proposed hypothesis in that the ODS alloy hoop performance can be improved via additional post-production deformation processes. At the outset significant grain alignment was recorded (Task 2.1. cross-rolling of flat MA956 samples) in the transverse direction for samples cross-rolled 20%. In the initial rotary cross rolling of MA956 tube samples we note a similar material flow in the circumferential direction as illustrated macroscopically via superficial markings in Figure 8 and via optical microstructural examination shown in Figure 9. Secondary deformation processes also seem to mitigate the occurrence of unrecrystallized fine-grained stringers, Figure 10(a), (b) that are extremely detrimental to hoop creep performance. We anticipate the material flow imposed in cross rolling and flow forming also acts to realign the remaining stringers in the hoop direction where there impact on creep void formation at these junctions can be mitigated as well.

This shear deformation imparted in cross rolling and its precise characteristics across the wall thickness of the tube are process dependent. This shear is surprisingly uniform across the tube wall thickness at $\beta=8^o$ and very non-uniform at $\beta=2^o$ cross rolling angle. For the initial trial at $\beta=2^o$ both forward and reverse rolling was performed during a single pass. Furthermore, the leading tube edge was not precisely tracked between passes, and it is unknown if this affects the overall sear deformation results. Nonetheless, the uniform shear observed at $\beta=8^o$ across the tube wall thickness illustrates the uniformity of the rotary rolling process under proper and well defined process parameters. Creep tests on rotary cross rolled ($\beta=8^o$) materials indicate a small

but consistent and reproducible hoop creep enhancement. The installation of an in-house rotary rolling apparatus at UCSD has been accomplished. The increased deformation capacity, on account of the larger power source, assures that materials can be rotary cross-rolled at ambient temperatures. This is beneficial in order to preserve the deformation strain energy that could produce large grains during its release upon recrystallization

Our initial intent was to compile creep data on cross-rolled samples to be compared to base data generated at Oak Ridge National Laboratory (ORNL). However, reference MA956 data from ORNL was compiled form samples with a different processing history. In an effort towards uniformity our own base hoop creep data for as received 2 ½"OD, ¼" wall thickness tubes is recorded in Table 2 and 3. The performance of flat MA956 cross-rolled 20% is also significantly improved as the creep rates are about 2 orders of magnitude better than the reference samples.

The creep performance enhancement is ambient temperature flow formed materials is most significant. This is surprising as the flow forming does not impart any grain rotations as evidenced in Task 2 or Task 3. However, the extreme cold working does affect secondary recrystallization and consequently produces coarse grain structures[10]. The flow formed creep results obtained exhibit some scatter perhaps due to the residual curvature in the room-temperature flattened specimens. On occasion such specimens exhibited large creep rates (for example test# 10). Results from flow formed materials recrystallized under the revised heat treatment (Air2) exhibited significant hoop creep enhancement over and above all previous iterations and trials. This suggests that optimum effects may be achievable via increased deformation strains alone. Furthermore, it appears that a 900^{o}C flattening treatment may not be detrimental as previously anticipated as it does not impede the development of the coarse grain structure. This result is expected to modify our processing path selection as the ***baseline MA956 tube material LMP = 46.09 has been improved to over 54.14 in hoop creep testing***. Such hoop creep performance in MA956 tubes beyond all previous results and has been demonstrated for the first time in this program.

§ 4. Conclusions

The current research program has demonstrated a consistent improvement in hoop creep response of ODS MA956 tubes made possible via a variety of post-production deformation techniques. This is the original predicate of our proposed program now being realized in practice.

We have successfully rotary cross-rolled while inducing significant and near uniform shear strain across the tube wall thickness under appropriate conditions. The grain shape changes and realignment are consistent with prior evidence for the flat cross-rolled samples. Creep tests of post processed samples via high temperature cross-rolling as well as the ambient temperature flow forming illustrate their significantly enhanced creep response in terms of creep rate/day as well as overall Larsen-Miller parameter when compared to baseline test results, see Table 2 and 3. Post-processing methods may be employed to improve the vendor-supplied material. Test results on flow formed MA956 (reduced 80-90% in wall-thickness) indicate that the creep performance is significantly enhanced at larger deformation strains. This beneficial improvement is considerably larger than that achieved in rotary or flat cross-rolled samples and is statistically significant. Result suggests that while the beneficial effects of grain shape control may become apparent at low deformation strains, these effects can be further improved upon with incremental deformation up to 80%. **Current test exposure for flow formed sample exceeds 7694 hours and 4200 hours for 2Ksi load creep tests at 975^{o}C and 1000^{o}C respectively.**

References:

1. F. Starr, in *Materials for High-Temperature Power Generation and Process Plant Applications*, A. Strang, Ed., IOM Communications Ltd., Book No. 728, pp. 79-152 (2000).

2. V.K. Sikka, I.G. Wright, and B.K. Kad, " Processing of Oxide-Dispersion-Strengthened Fe_3Al-Based Alloy Tube" (1998) *12th Annual Fossil Energy Materials Conf.*, Knoxville, TN, May 12-14, 1998, p.11-19

3. B.K. Kad, C.G. McKamey, I.G. Wright and V.K. Sikka, "Optimization of ODS-Alloy Properties" (2002) *16th Annual Fossil Energy Materials Conf.*, Baltimore, MD, April 22nd –24th, 2002.

4. B.K. Kad, C.G. McKamey, I.G. Wright and V.K. Sikka, "High Temperature Mechanical Properties of ODS-Fe_3Al Tubes" (2001) *15th Annual Fossil Energy Materials Conf.*, Knoxville, TN, April 30th -May 2nd, 2001

5. B.K. Kad, V.K. Sikka, R.N. Wright and I.G. Wright, "Oxide Dispersion Strengthened Fe_3Al-Based Alloy Tubes" (2000) *14th Annual Fossil Energy Materials Conf.*, Knoxville, TN, April 24-26, 2000; *ibid* (1999) *13th Annual Fossil Energy Materials Conf.*, Knoxville, TN, May 11th –14t, 1999.

6. J. Ritherdon, A.R. Jones and I.G. Wright, "The Recovery and Recrystallization of a Mechanically Alloyed ODS-Fe_3Al Alloy" (2001) *Materials Science Forum*, **360-362**, pp.217-222, 2001

7. I.W. Chen and A.S. Argon, "Creep Cavitation in 304 Stainless Steel" (1981) *Acta Metallurgica*, **29**, p.1321, 1981; *ibid.* "Diffusive Growth of Grain-Boundary Cavities" *Acta Metallurgica*, **29**, p1759, 1981

8. B.K. Kad, I.G. Wright, V.K. Sikka and R.R. Judkins, (2004) "Optimization of Hoop Creep Response in ODS-Fe_3Al Tubes" *18th Annual Fossil Energy Materials Conf.*, Knoxville, TN, June 2nd – 4th, 2004

9. T.Z. Blazynski, "Metal Forming – Tool Profiles and Flow" Macmillan Press, NY, 1976

10. C. Capdevila and H.K. Bhadeshia, 'Manufacturing and Microstructural Evolution of Mechanically Alloyed Oxide Dispersion Strengthened Superalloys', Advanced Engineering Materials, 2001, 3(9), 647.